RSC Advances

PAPER

View Article Online
View Journal | View Issue

Cite this: *RSC Adv.*, 2020, **10**, 35765

A sandwich-type bacteriophage-based amperometric biosensor for the detection of Shiga toxin-producing *Escherichia coli* serogroups in complex matrices†

Irwin A. Quintela and Vivian C. H. Wu *

Immuno-based biosensors are a popular tool designed for pathogen screening and detection. The current antibody-based biosensors employ direct, indirect, or sandwich detection approaches; however, instability, cross-reactivity, and high-cost render them unreliable and impractical. To circumvent these drawbacks, here we report a portable sandwich-type bacteriophage-based amperometric biosensor, which is highly-specific to various Shiga toxin-producing *Escherichia coli* (STEC) serogroups. Environmentally isolated and biotinylated bacteriophages were directly immobilized onto a streptavidin-coated screen-printed carbon electrode (SPCE), which recognized and captured viable target cells. Samples (50 μL) were transferred to these bacteriophage-functionalized SPCEs (12 min, room temp) before sequentially adding a bacteriophage–gold nanoparticle solution (20 μL), H_2O_2 (40 mM), and 1,1′-ferrocenedicarboxylic acid for amperometric tests (100 mV s^{-1}) and analysis (ANOVA and LSD, $P < 0.05$). The optimum biotin concentration (10 mM) retained 94.47% bacteriophage viability. Non-target bacteria (*Listeria monocytogenes* and *Salmonella* Typhimurium) had delta currents below the threshold of a positive detection. With less than 1 h turn-around time, the amperometric biosensor had a detection limit of 10–10^2 CFU mL^{-1} for STEC O157, O26, and O179 strains and R^2 values of 0.97, 0.99, and 0.87, respectively, and a similar detection limit was observed in complex matrices, 10–10^2 CFU g^{-1} or mL^{-1} with R^2 values of 0.98, 0.95, and 0.76, respectively. The newly developed portable amperometric biosensor was able to rapidly detect viable target cells at low inoculum levels, thus providing an inexpensive and improved alternative to the current immuno- and laboratory-based STEC screening methods.

Received 17th July 2020
Accepted 15th September 2020

DOI: 10.1039/d0ra06223e

rsc.li/rsc-advances

1. Introduction

Shiga toxin-producing *Escherichia coli* (STEC) has been a significant cause of periodic and epidemic foodborne diseases such as gastroenteritis, hemorrhagic colitis (HC), and hemolytic-uremic syndrome (HUS).[1–3] An estimate of 110 000 cases is reported each year, ranging from mild diarrhea to HUS (10%), and a recent multi-state prospective study showed 259 children had HUS as a complication of STEC O157:H7 infection.[4,5] HUS is one of the primary causes of acute kidney injury (AKI), especially in pediatric patients.[1,6] Rapid and accurate screening of STEC using highly selective and easy-to-operate tools is one of the most efficient approaches to reduce the incidence of illnesses and hospitalizations through contaminated food products. Early detection and the ability to precisely screen pathogenic microorganisms prevent potential massive product recalls and incurring a severe economic loss.

Research focus in the field of detection of pathogenic bacteria has been geared towards the development of on-site sensor devices.[7] Researchers are developing affordable and on-site systems that are aimed to move away sample processing and testing from a centralized laboratory.[8] In the field of immunoassays, the common antibody–antigen interactions in enzyme-linked immunosorbent assay (ELISA) and agglutination kits for the detection of foodborne pathogens are relatively easier to perform but often generate false-positive results and are not capable of differentiating viable from non-viable cells.[9,10] Antibodies are commonly integrated as bioreceptors and capture elements with biosensors due to their high affinities to specific targets.[11] Binding fragments are also relatively easy to modify using protein engineering and are widely utilized in nanotechnology applications.[12] Foodborne pathogens such as STEC O157:H7, *Salmonella* spp., *Vibrio* spp., and viruses have been detected by antibodies-based biosensors coupled with various transducers and techniques such as

Produce Safety and Microbiology Research Unit, US Department of Agriculture, Agricultural Research Services, Western Regional Research Center, Albany, California, USA. E-mail: vivian.wu@usda.gov

† Electronic supplementary information (ESI) available. See DOI: 10.1039/d0ra06223e

chemiluminescence,[13] electrochemiluminescence and fluorescence,[14] QCM immunosensor,[15] SAW,[16] differential pulse voltammetry,[17] evanescent wave fiber-optic assay,[18] lateral-flow assay,[19] and SPR.[20]

However, though polymerase chain reaction (PCR)-based method can improve the sensitivities of immunoassays (approximately 100-fold), it requires thermocycling platforms, trained staff, and reliable infrastructures which can be challenging in areas with scarce resources.[21] Another drawback of molecular or nucleic acid amplification techniques (*i.e.*, PCR) is its destructive nature or the need to break up the cells. In occasions when rare cells are encountered, it would require more than a single test to be carried out; then, it becomes a limiting factor.[22]

Due to the inherently long turn-around time of conventional pathogen detection methods, biosensors are specifically designed to significantly reduce the processing time between sample uptake and test results at a fraction of the cost of conventional methods. It has been found in the published scientific literature that biosensor ranks as the fourth most popular method and the fastest growing technology in the area of pathogen detection.[23] It is comprised of target or analytes-specific biorecognition or bioreceptor elements and a physiochemical transducer that converts and relays signals to an amplifier and computer.[24,25] However, it is important to note that the continuous emergence of rapid pathogen detection necessitates a thorough understanding of the major differences among devices according to the molecular interactions between the target analyte and biorecognition agents for efficiency.[26]

Bacteriophages possess excellent host selectivity and have been used as biorecognition elements for pathogen detection.[27] The receptor-binding proteins of bacteriophages recognize bacterial host cells and subsequently inject nucleic acids in the host-cell cytoplasm. Bacteriophages are present in the natural environment and are inexpensive to propagate, and thus are excellent alternatives to antibodies as biological recognition receptors. More importantly, bacteriophages are highly host-specific and very stable, allowing easy handling and storage. Previous studies utilized bacteriophages as biosensor recognition elements, or capture elements for the detection of pathogens such as *Salmonella* spp.,[28,29] *Listeria* spp.,[30] *Staphylococcus aureus*,[31] and *E. coli*.[32] However, the majority of the published study on bacteriophage-based biosensors did not achieve an excellent detection limit (10^3 CFU mL^{-1} was reported) even in pure culture setup. This could be attributed to the design of the detection system and the platforms that were utilized. Many of these detection systems employed single-binding event between the biorecognition or capture element of the biosensors and target analyte(s). Though bacteriophages have shown high-specificity toward its bacterial, incorporating bacteriophages onto the detection system as the biorecognition elements may need a secondary binding event to enhance sensitivity, specificity, and reliability. A secondary binding event is often employed in dual-site binding assay or known as a sandwich assay. With these two layers of recognition, the performance of bacteriophage-based can be greatly improved even when used in a more complicated setup and testing various complex matrices. None of the reported bacteriophage-based detection technology employed bacteriophages (two of the same kind) for sandwich capture and detection of viable target bacterial cells. Therefore, here we report a novel approach by utilizing bacteriophages as both capture and detection elements to construct an electrochemical biosensor for STEC detection and achieve an improved detection limit. The primary aim of this study was to develop a sandwich-type bacteriophage-based amperometric biosensor for STEC serogroups and apply the biosensor directly on complex matrices.

2. Experimental methods

2.1. Chemical reagents and apparatus

Phosphate-Buffered Saline (PBS, 10×), Pierce™ 20× TBS Tween™ 20 buffer (TBS-T20), biotin, sulfo-*N*-hydroxysulfosuccinimide (NHS), streptavidin, potassium ferricyanide $K_3[FeCN_6]$], 30% hydrogen peroxide (H_2O_2), dimethyl sulfoxide (DMSO) solvent, sulfuric acid, ethyl alcohol, Pierce™ Protein-Free Blocking Buffer, polyethylene glycol (PEG), Blocker-Casein blocking buffer, Pierce™ BCA Protein Assay Kit (Thermo Fisher Scientific, Wilmington, DE, USA), sulfosuccinimidobiotin (EZ-Link™ Sulfo-NHS-Biotin), Zeba™ Spin Desalting Columns, 4′-hydroxyazobenzene-2-carboxylic acid (HABA), and streptavidin-coated nanocrystals Qdots (QDs) were purchased from Thermo Fisher Scientific (Waltham, MA). *N*-(3-Dimethylaminopropyl)-*N*′-ethylcarbodiimide hydrochloride (EDC), carboxymethyl dextran (CMD) sodium salt, horseradish peroxidase (HRP)-conjugated streptavidin (S-HRP), and bovine serum albumin (BSA) were purchased from Sigma-Aldrich (St. Louis, MO). 1,1′-Ferrocenedicarboxylic acid (FeDC) was purchased from Strem Chemicals (Newburyport, MA). A solution of gold nanoparticles (AuNPs) with an average diameter of 13 nm was prepared as previously reported.[3] Unmodified disposable SPCEs (cat. no. DRP-110, DRP-C110) with three electrodes, a circular carbon working electrode (4 mm), a carbon counter electrode, and a silver reference electrode on a ceramic substrate (34 × 10 × 0.5 mm) were purchased from DropSens (Asturias, Spain). Electrochemical measurements were conducted using PalmSens3 electrochemical portable potentiostat/galvanostat/impedance analyzer (PalmSens, Houten, The Netherlands) that was wirelessly connected *via* Bluetooth™ and controlled by PSTrace5 software (PalmSens) installed on an Android™ device.

2.2. Bacterial strains and bacteriophages

The bacteriophages used in this study were originally isolated from environmental samples and stored at the USDA-Agricultural Research Services Center-Produce Safety and Microbiology Unit, (Albany, CA) belonging to *Siphoviridae* and *Myoviridae* families. Representative strains of STEC serogroups, O26:H11 HH8, O157:H7 ATCC 35150, and O179, were utilized as target bacteria. *Salmonella* Typhimurium ATCC 14028 and *Listeria monocytogenes* ATCC 19115 were used as non-target groups. All bacterial strains were obtained from the collections of the University of Maine-Pathogenic Microbiology

Laboratory (Orono, ME) and the USDA Agricultural Research Services (ARS)-Produce Safety and Microbiology Unit in Albany, CA and USDA ARS in Wyndmoor, PA. Bacterial cells frozen in cryogenic beads (CryoSavers; Hardy Diagnostics, Santa Maria, CA, USA) were activated and revived in Brain Heart Infusion (BHI) broth (Neogen, Lansing, MI, USA) at 37 °C. Overnight cultures were washed in 10 mL of 1× PBS by centrifugation at 5000 × *g* for 10 min. Pellets were resuspended in 1× PBS and serially diluted up to $1:10^7$. MacConkey Agar with sorbitol, xylose lysine deoxycholate agar, and PALCAM agar (all from Neogen) were used for STEC strains, *S.* Typhimurium, and *L. monocytogenes*, respectively.

Titer levels (PFU mL^{-1}) of STEC-specific bacteriophages were determined by a plaque assay. In brief, 100 μL of serially diluted bacteriophage suspensions were mixed with overnight host bacterial cultures (200 μL) and molten tryptic soy agar (5 mL, Neogen) before pouring the mixture into plates and incubated at 37 °C overnight.

2.3. Chemical modification of bacteriophages

Bacteriophage stock solutions (μg mL^{-1}) at various concentrations were biotinylated with sulfosuccinimidobiotin (1–20 mM) and incubated at 4 °C overnight before dialysis against 1× PBS using Zeba™ Spin Desalting Columns to remove excess and unbound biotin. To determine the concentration of bacteriophages, a standard curve based on absorbance (562 nm) was generated by following the manufacturer's instructions (Pierce™ BCA Protein Assay Kit). Incorporated biotin was measured by the spectrophotometric HABA assay at 500 nm absorbance. To monitor the effects of biotin, biotinylated bacteriophages were coupled with streptavidin-coated QDs and viewed under a transmission electron microscope (TEM; FEI Tecnai G2 F20).[33] In brief, 2 μL of biotinylated bacteriophage–QDs solution was dropped onto carbon-coated formvar films on copper grids. After negative staining using 1.5% uranyl acetate (pH 4–4.5), the samples were air-dried and viewed under the TEM at 200 kV. To determine the optimum concentration of biotin, the maximum viability retention of bacteriophages was investigated by plaque assays pre and post biotinylation.

2.4. Electrochemical behavior and characterization of screen-printed carbon electrodes (SPCE)

Unmodified SPCEs were characterized by recording cyclic voltammograms of 0.5 mM $K_3[Fe(CN_6)]$ in two separate supporting electrolytes, 0.1 M H_2SO_4, and 1× PBS at increasing scan rates (50, 100, 200, and 500 mV s^{-1}) under −500 mV to +500 mV *vs.* counter/reference electrode potential step. Oxidation and reduction peak potentials from the scans were used to identify peak separation ΔE_p ($\Delta E_p = E_p^c - E_p^a$, where E_p^c is the cathodic peak and E_p^a is anodic peak) of the redox system. To characterize the behaviors of SPCE post modifications, all reagents were individually tested with the cyclic voltammetry (CV) probe, $K_3[Fe(CN_6)]$. In brief, reagents (20 μL) including CMD, EDC-NHS, streptavidin, biotinylated bacteriophages, FeDC, AuNP, BSA, casein, protein-free blocking reagents, and PEG were dropped individually onto SPCEs, air-dried, and tested with 0.5 mM $K_3[Fe(CN_6)]$ at 100 mV s^{-1}.

2.5. Bacteriophage-based capture and detection elements

To introduce carboxyl (–COOH) onto the clean working electrode surface, CMD was added (50 mg mL^{-1}) and kept in an orbital shaker at room temperature (25 °C) for 3 h. An equal volume of EDC (0.4 M) and NHS (0.1 M) was added to activate –COOH. Amine-carrying streptavidin (50 μg mL^{-1}) was added and incubated for 40 min to allow carboxyl-to-amine cross-linking. After removing the excess liquid, modified SPCEs were stored in humidified containers before adding biotinylated bacteriophages (>10^9 PFU mL^{-1}) and incubation at 4 °C overnight. Biofunctionalized SPCEs were blocked with 30% casein (20 μL) at 4 °C overnight, washed twice with TBS-T20, and once with 0.5× PBS prior to storage at 4 °C. Each set of biofunctionalized SPCEs was specific to each of the three STEC serogroups. The capture element refers to biofunctionalized SPCEs and is used hereafter. The bioactivity of the capture element was evaluated after 48 h using an agar diffusion method. Cyclic voltammograms of capture elements and unmodified SPCEs were compared at 100 mV s^{-1} with 0.5 mM $K_3[Fe(CN_6)]$.

In constructing the detection element solution, biotinylated bacteriophages were mixed with streptavidin-HRP (100 μg mL^{-1}) and AuNP solution (20 μM) and incubated overnight at 4 °C. The viability of bacteriophages was evaluated by conducting the plaque assay and viewing under TEM. All reagents in the biosensor assembly were investigated for noise that contributed to the background signal of the system. In brief, 20 μL of each reagent was added onto clean SPCEs, which were then incubated for 30 s before subjecting to by amperometric tests.

2.6. Electrochemical tests of pure STEC strain cultures and detection limit

Serially diluted STEC samples (50 μL, 10–10^4 and 10^8 CFU mL^{-1}) or control (50 μL, 1× PBS) were added onto the functionalized SPCEs, which were then incubated at room temperature (25 °C, 12 min) and washed with 0.5× PBS. Detection element solution (20 μL) was incubated for 10 min, washed twice with TBS-T20 and 0.5× PBS. The mediator (5 μL, 250 mM FeDC in DMSO) was added for 30 s, followed by the addition of H_2O_2 (40 mM) for another 30 s. Then amperometry was performed at room temperature (25 °C), with a fixed potential of 0.5 V throughout the trial, 0.5 s interval, and 100 s run time. All samples were analyzed in triplicates. The response currents (RC, μA) within a set of potentials over time were measured. Delta (Δ) current, [Δ current = RC of sample (target or non-target) − RC of control] was used to determine the specificity and sensitivity of the assay, with the signal threshold for positive detection defined as a signal-to-noise (S/N) ratio of > 2, wherein the target generated a signal a least two times greater than that from non-target samples. The linear calibration curve ($y = mx + b$) assumed the response (y) is linearly related to the concentration (x). The detection limit was determined by the statistical significance of

the difference of signals (Δ current) between non-target bacteria and the lowest inoculum of target bacteria that had Δ current above the signal threshold for positive detection.

2.7. Detection of STEC strains in artificially inoculated and natural complex matrices

Fresh ground beef and pasteurized apple juice were purchased from a local retail store. In brief, weighed fresh ground beef samples (25 g) were transferred into individual stomacher bags (Thermo Fisher Scientific). Overnight bacterial cultures were washed, diluted, and individually spiked on fresh ground beef samples (25 g) to reach the desired final inoculum levels of 10–10^4 and 10^8 CFU g^{-1} or mL^{-1}, followed by 10 s of homogenization using a Pulsifier (Microbiology International, MD, USA) at a low setting. For pasteurized apple juice, 1 mL of inoculum was added into 9 mL of sample and then diluted to obtain the same inoculum levels as the fresh ground beef samples. For both food matrices, 1× PBS was used as a blank, and *S.* Typhimurium ATCC 14028 was used as a non-target sample.

Natural environmental water samples were collected from ponds and water trough used to irrigate fields and farms with observed animal activities (*i.e.*, coyote and deer tracks) (Table S1†). Fifty milliliters of liquid samples were used for testing, while conventional PCR targeting *stx* genes and the standard plate count method (Table S2†) were conducted for parallel comparison and verification.

2.8. Statistical analysis

Each experiment was conducted on three separate occasions in triplicates. Data were reported as the mean ± S.D. and analyzed by one-way analysis of variance followed by Fisher's least significance difference post-hoc tests using JMP software (Cary, NC, USA). $P < 0.05$ was considered significant.

3. Results and discussion

The detection principle of the developed bacteriophage-based amperometric biosensor is shown in Fig. 1 and the complete system architecture is presented in Fig. S1.†

The key novel feature of the sensor presented here is the bacteriophage-based capture and sandwich-type detection of viable target cells. The majority of functional receptors of bacteriophages are located on its tail extremities. Sulfosuccinimido-biotin was used to modify the bacteriophage heads as it reacted with the primary amino groups of the coat proteins concentrated on the bacteriophage heads.[28] This modification resulted in an oriented immobilization of the bacteriophages, wherein the tails are directed upward and allows efficient target recognition and capture.[34] Once STEC cells were captured by the immobilized bacteriophages, the detection element solution was added, which was comprised of the same bacteriophages but labeled with HRP to accelerate the catalytic reaction and conjugated with AuNPs to amplify signals. The addition of the detection element solution allowed sandwich capture of STEC cells and specific bacteriophage-host binding events. After bacteriophage/STEC/bacteriophage-S-HRP complex formation, a mixture of 40 mM H_2O_2 and FeDC was added onto the SPCEs. H_2O_2 served as a substrate for HRP, whereas FeDC acted as a mediator, shuttling electrons between the redox reaction center and the working electrode.[35] Horse-Radish Peroxidase (HRP) has been previously used to label long tail fiber proteins of bacteriophages S16 to construct a highly specific and sensitive probe for *Salmonella* spp. HRP-catalyzed detection assay.[36] Moreover, three STEC bacteriophages that can infect O26, O103, O111, O145, and O157 serogroups were chemically labeled with HRP for luminescence-based assay.[37] The high binding efficiency of the HRP-labeled bacteriophage to the host cells resulted in high biosensor sensitivity. To our knowledge, this is the first study to use two sets of same bacteriophages for sandwich capture and detection

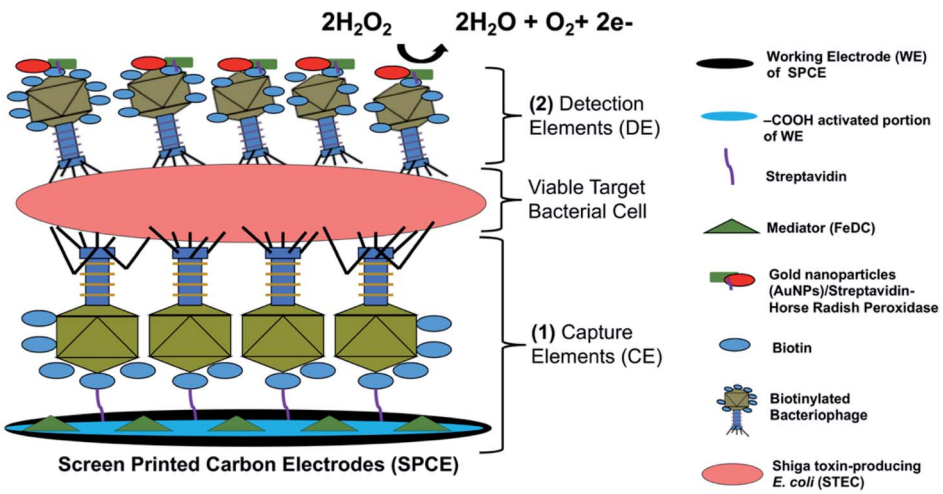

Fig. 1 The detection principle of the bacteriophage-based functionalized SPCE biosensor. Two sets of highly specific biotinylated bacteriophages were used as (1) SPCE-bound capture element and (2) AuNP–S-HRP-tagged detection element binding to captured viable STEC cells for peroxidase-coupled SPCE redox reactions.

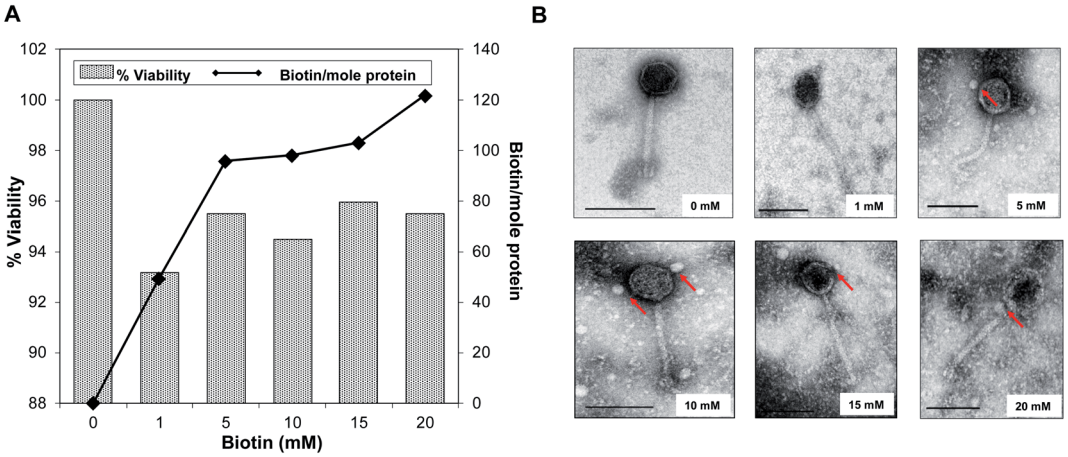

Fig. 2 Biotinylation and viability of STEC O179 bacteriophage. (A) The effects of biotinylation in relation to bacteriophage viability. (B) TEM images of biotinylated bacteriophages with increasing biotin concentrations (0 mM–20 mM) and coupling it with streptavidin-coated QDots. Scale: 100 nm.

of viable target bacterial cells. An excellent biorecognition element is highly durable, easy to immobilize, cost-efficient, and highly selective and sensitive.[31] These key attributes are fulfilled by bacteriophages, both as biorecognition for capturing and reporting viable STEC cells.

3.1. Viability of chemically-modified bacteriophages

The effects of biotinylation on the bacteriophage viability at 10^{10} PFU mL^{-1} titer level is shown in Fig. 2A. The occurrence of biotinylation of bacteriophage head was at its lowest level (49.37 biotin per mole protein) when 1 mM biotin was introduced and was doubled when 5–10 mM range was used (95.71–98.15 biotin per mole protein). The highest concentration of incorporated biotin was 121.92 biotin per mole protein with 20 mM biotin. Viability and infectivity remained high even after chemical biotinylation (94.47%). Fig. 2B shows morphological observation after biotinylation by tracking bound streptavidin-coated Qdots to bacteriophage head. Within 5–15 mM biotin concentrations range, no major morphological changes were observed while the thickening of head and denser capsid at 20 mM biotin was obvious. Data showed that the optimum biotin concentration range was within 10–15 mM range; thus 10 mM was selected was in the subsequent procedures.

3.2. Characterization and behavioral analysis of unmodified SPCEs

Cyclic voltammetry of $K_3[Fe(CN_6)]$ was conducted in two supporting electrolytes, 0.1 M H_2SO_4 (Fig. 3A) and 1× PBS (Fig. 3B), at varying scan rates. The peak potential separation values (ΔE_p) increased with scan rate; for 0.1 M H_2SO_4, ΔE_p was 243.2 mV at 200 mV s^{-1} and 324.3 mV at 500 mV s^{-1}. A similar increasing trend was observed for 1× PBS; ΔE_p was 170.6 mV at 200 mV s^{-1} and 216.2 mV at 500 mV s^{-1} (Fig. S2, Table S3†). The supporting electrolyte did not participate in any electrode reactions; however, it increased the conductivity of the solution.[38] Salt as a supporting electrolyte ensures high ionic strength (0.1 M), thus maintaining a homogenous and near-zero electric field that shields the solution from redox reactions of the target analytes and reduces electrode resistance to a negligible level.[39,40] Similarly, sulfuric acid reduces the electric field in the solution as well as the transport of cupric ions.[38] 1× PBS generated lower ΔE_p than H_2SO_4; therefore, it was used in the subsequent characterization of SPCEs at a scan rate of 100 mV s^{-1}, as low ΔE_p values indicated an excellent quality of the electrode surfaces as well as optimal parameter settings (*i.e.*, scan rate). It was also found that 50 mV s^{-1} scan rate generated the lowest current, irrespective of the supporting electrolyte. However, at 100 mV s^{-1}, the current was consistent and stable during cyclic voltammetry and amperometric tests.

3.3. Biofunctionalization of SPCEs

In Fig. 3C unmodified SPCEs showed higher cathodic peaks (E_p^c) than chemically modified SPCEs. The blocking features of the chemicals may have affected the electron transfer kinetics of the redox probe. Casein, known as an excellent blocking reagent, had the lowest E_p^c, and may have effectively blocked the SPCE surfaces, as observed from the voltammogram produced from SPCEs generated using casein (light blue curve) in comparison with those of SPCEs generated using other blocking reagents. In Fig. 3D, it can be observed that voltammograms generated from unmodified and modified-biofunctionalized SPCEs are clearly distinct with ΔE_p values of 201.02 mV and 393.60 mV, respectively. This difference (ΔE_p) indicates a successful modification of SPCEs by coating and layering with various components onto the surface of the working electrode while retaining its stability even after several incubating and washing steps. Additional data on the modification of SPCEs are presented in Table S4.†

Modified SPCEs generated lower currents than the unmodified counterpart, primarily due to the blocking property of the working electrode surface. A properly ordered self-assembled monolayer of small molecules allows electron transfer from the solution to the electrode. The lack of a peak in the

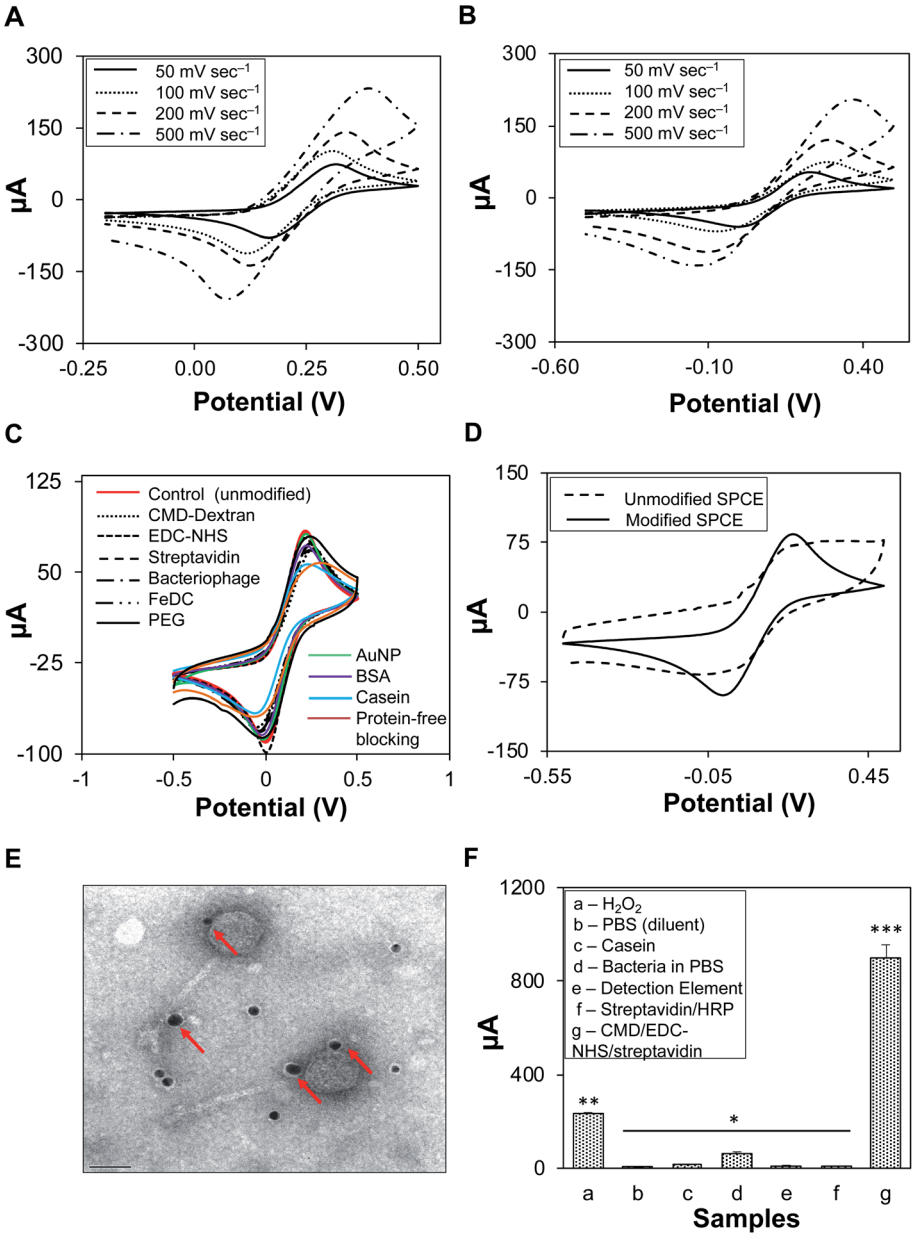

Fig. 3 Development and optimization of capture and detection elements. $K_3[Fe(CN_6)]$ (0.5 mM) was used with (A) 0.1 M sulfuric acid or (B) 1× PBS as a supporting electrolyte at increasing scan rates. (C) Cyclic voltammograms (100 mV s^{-1}) of chemical reagents. (D) Cyclic voltammogram of unmodified and modified SPCEs. (E) TEM image of the detection element solution, AuNPs (signal amplifiers) seen as dark spots (indicated by arrows) were bound to biotinylated STEC O179 bacteriophages. (F) Determination of sources of background noise by amperometry. Background signal approximately 900 μA (896 ± 58.24 μA) was determined and used as the baseline value to analyze subsequent amperometric tests. Bars with different asterisks (*) are significantly different ($P < 0.05$).

voltammograms of monolayer-modified SPCEs indicated that redox reactions did not occur. Reductions in the voltammetric response were observed in all modification steps, *i.e.*, after the addition of individual reagents and when the actual linkages were assembled. CMD was added onto the SPCE surface to introduce carboxyl groups and was activated by the addition of EDC–NHS. This self-assembled monolayer was terminated with an active amine-carrying streptavidin *via* carboxyl-to-amine crosslinking, and ultimately covalently bonded with the biotinylated bacteriophages. These surface layers hindered the diffusion of redox probe toward the electrode surface, indicating efficient and successful immobilization and modification of the SPCE surface.[41] After functionalization, the stability and viability of immobilized biotinylated bacteriophages (STEC O179) were evaluated by the agar diffusion method (Fig. S3†). STEC O179 bacteriophage showed zones of clearing, indicating stable immobilization, biofunctionality, and biocompatibility with the electrodes.[42] The bacteriophages that were included in this study belong to families *Siphoviridae* and *Myoviridae*. Both families have been reported to be highly resistant to long-term

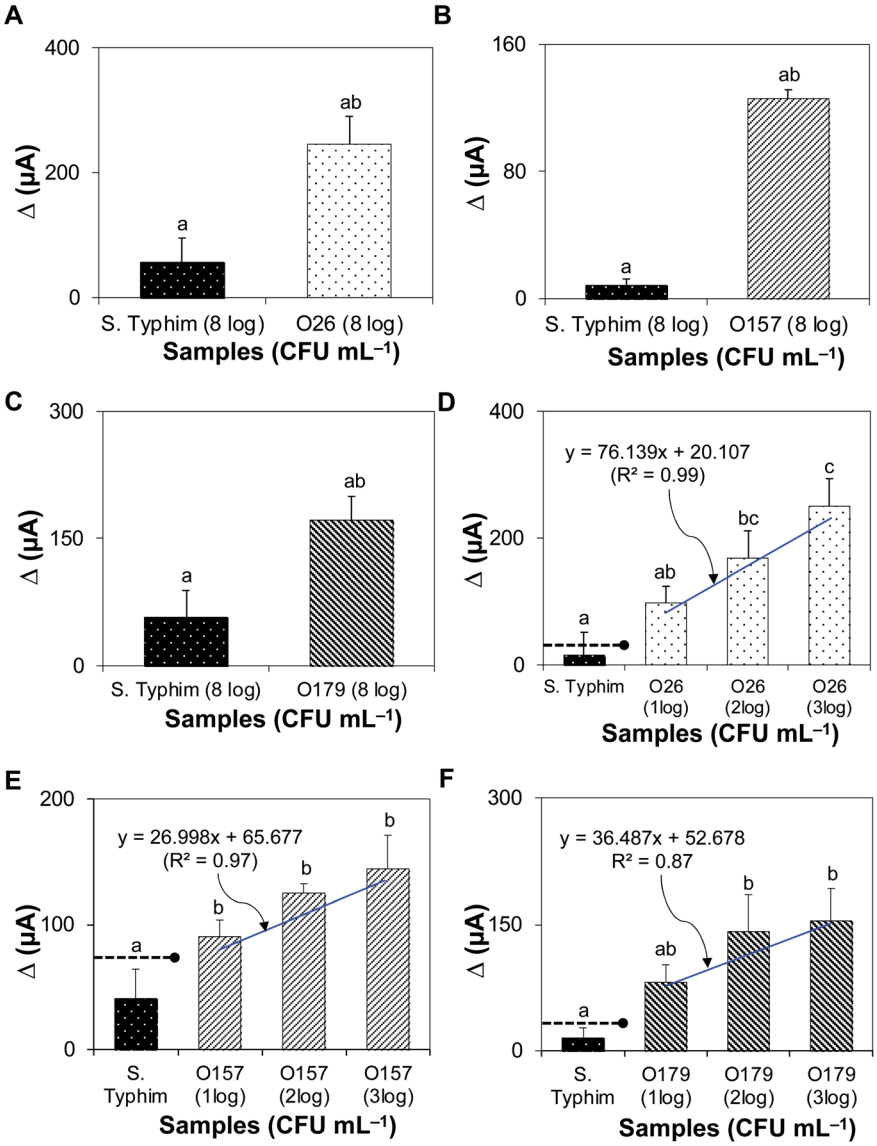

Fig. 4 Specificity and sensitivity of the biosensor in a pure culture set up. (A–C) The specificity of the assay was challenged by testing and comparing Δ currents between target STEC bacteria and non-target samples (*S.* Typhimurium). (D–F) The sensitivity of the assay was tested from 10 to 10^3 CFU mL^{-1} of target STEC (O26, O157, and O179). The threshold of (+) detection was defined by the signal-to-noise (S/N) characteristics as S/N > 2. Dashed lines with solid circles indicate the threshold for positive detection. Bars with different lower-case letters are significantly different ($P < 0.05$). The detection limit was determined by the statistical significance of Δ current between non-target bacteria and the lowest inoculum of target bacteria that had Δ current above the signal threshold for positive detection.

storage, dry conditions, and large temperature fluctuations.[43] Chemical modification was chosen over other techniques for SPCE functionalization because of the ease and simplicity of this approach. Active chemical modification of the SPCEs with streptavidin allowed tethering of biotinylated bacteriophages *via* the strong streptavidin–biotin interaction. The stability and viability of bacteriophages indicated that the biotinylated bacteriophages were strongly linked to the surface of the working electrode *via* biotin-streptavidin bonds rather than physical adsorption, as most of the bacteriophages would have been washed away during the washing steps. Previous bacteriophage immobilization techniques involved passive,[44] charge-directed oriented immobilization,[45,46] and chemical immobilization *via* streptavidin on quantum dots.[33] Passive immobilization resulted in poor cell capture efficiency,[34] while chemical immobilization involved genetically-modified bacteriophages, which are not always economical, especially for a comprehensive collection of environmental and genetically uncharacterized bacteriophages.

3.4. Development of bacteriophage-based detection elements with signal amplifiers

Detection element solution containing biotinylated bacteriophage/S-HRP/AuNP complex was viewed under the TEM. Gold nanoparticles as signal amplifiers can be seen as dark spots and were

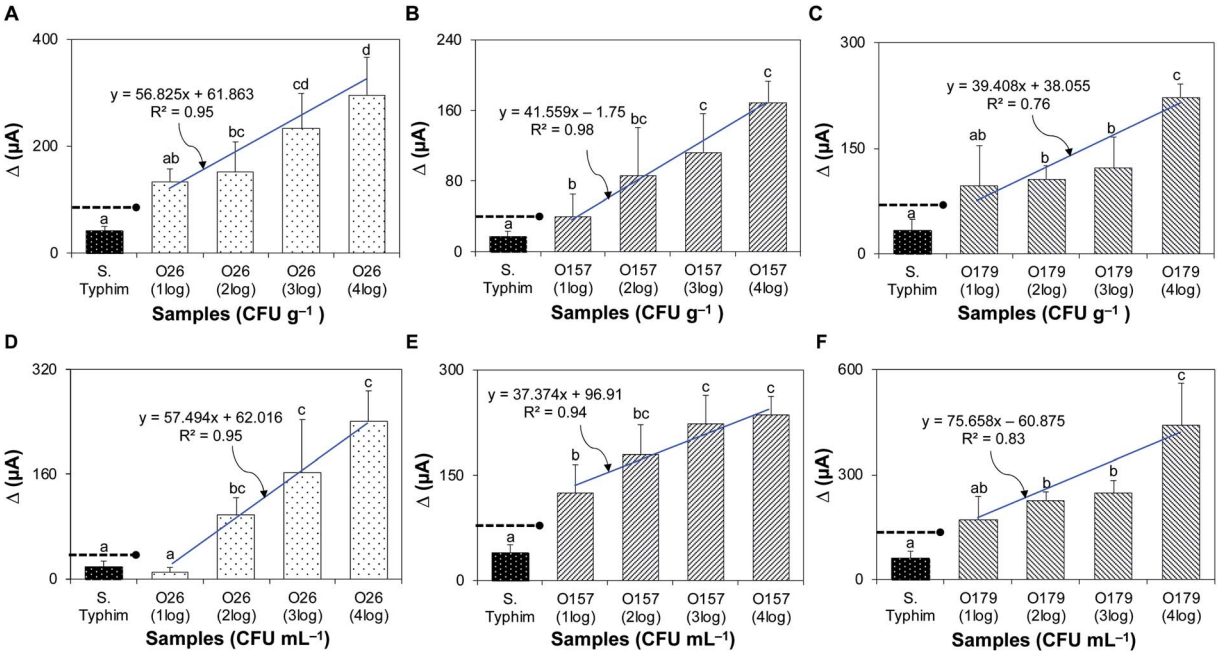

Fig. 5 Detection of STEC strains in artificially inoculated complex matrices. (A–C) Bar graphs showing the sensitivity of detection for STEC O26, O157, and O179 in the fresh ground beef matrix. (D–F) Bar graphs showing the sensitivity of detection for STEC O26, O157, and O179 in pasteurized apple juice. Dashed lines with solid circles indicate the threshold for positive detection. Bars with different lower-case letters are significantly different ($P < 0.05$). The detection limit was determined by the statistical significance of Δ current between non-target bacteria and the lowest inoculum of target bacteria that had Δ current above the signal threshold for positive detection.

bound to the biotinylated STEC O179 bacteriophages (Fig. 3E). Most of the attached AuNPs were observed along with the heads and tails of the bacteriophages, but not directly to the tail fibers, which could have blocked the specific binding of bacteriophages to host cells. Gold nanoparticles (AuNPs) are widely utilized as signal amplifiers because they are biocompatible, have synergistic effects on catalytic activity, promote electron transfer between mediators and electrodes, and have a large electrochemically active surface.[35,47,48] Other nanomaterials and nanosheets such as nickel nanoparticles (NP) and graphitic carbon nitrides (gC_3N_4) have also attracted attention for potential applications due to their surface area and excellent electron transportability.[49,50] The infectivity of biotinylated bacteriophages in the detection element solution was not negatively affected by the binding of AuNPs.

3.5. Individual reagents as sources of background noise

Sources of noise and indirect signals are presented in Fig. 3F. Reagents were classified into three major groups based on their functionality. The response currents (μA) for individual reagents that could have indirectly interfered with the signal and ultimately contributed to the background noise of the system were measured. The results showed that response currents from reagents and detection elements were mostly negligible, except for that of H_2O_2 (230.66 ± 6.32 μA). Modified SPCEs (CMD/EDC–NHS/streptavidin) had the strongest response current detected, 896.51 ± 58.24 μA. Based on these findings, the baseline response value was set at 900 μA, which was applied to subsequent amperometric measurements. The dimension of the working electrode strongly influenced the noise and stability of the sensor, such as the noise was directly proportional to the electrode area.[51,52] Though the working electrode had a diameter of only 4 mm, the transducer-induced noise highly likely originated from the thermal motion of ions in the electrolyte–electrode interface where electrode pores created a frictional environment.[53] Another possibility was power line interference pickup, which contributed to the overall background noise; therefore, it was recommended to insulate all microelectrode connections.[53]

3.6. Electrochemical detection of pure STEC strain cultures

Fig. 4A–C shows that the bacteriophage-based biosensor was highly-specific. Delta (Δ) currents of all target bacteria tested were significantly higher than those of non-target samples. The sensitivity of the assay is presented in Fig. 4D–F; the detection limits for STEC strains O26, O157, and O179 were 10^2, 10, and 10^2 CFU mL^{-1}, with R^2 values of 0.99, 0.97, and 0.87, respectively.

3.7. Detection of STEC strains in artificially inoculated and natural complex matrices

Solid and liquid food samples (fresh ground beef and pasteurized apple juice) were tested without pre-treatment. The device detected STEC strains O26, O157, and O179 in ground beef, with detection limits of 10^2, 10, and 10^2 CFU g^{-1} and R^2 values of 0.95, 0.98, and 0.76, respectively (Fig. 5A–C), and in pasteurized apple juice, with detection limits of 10^2, 10, and 10^2 CFU mL^{-1} and R^2 values of 0.95, 0.94, and 0.83, respectively (Fig. 5D–F).

Fig. 6A–C show the results for the environmental water samples. The Δ current (μA) for each sample was compared to

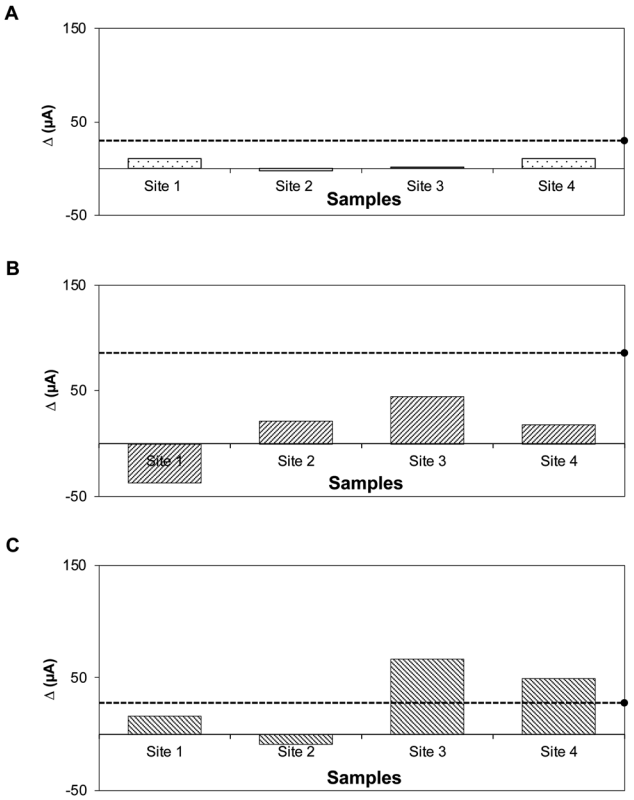

Fig. 6 Detection of STEC strains in natural environmental water samples. The natural environmental water samples were collected at four different sites. Bar graphs showing Δ currents (μA) for (A) STEC O26, (B) STEC O157, and (C) STEC O179. Dashed lines with solid circle indicate the threshold for positive detection established in pure culture setup.

the threshold for positive detection established from pure cultures. Water samples tested negative and had generated Δ current (μA) below the positive threshold for STEC O26 and O157. For STEC O179, Δ currents for samples from sites 3 and 4 were slightly above the positive threshold. However, parallel tests showed negative; the standard plate method using selective media and PCR for *stx* genes showed that none of the environmental water samples contained the virulence gene-specific for STEC serogroups (Fig. S4 and S5). This difference could be attributed to the generated signals, which were below the reference detection limit in pure culture for STEC O179 (10^2 CFU mL^{-1}, Δ current = 141 μA).

The results of this study strongly suggested that antibody-free portable detection systems allowed the rapid detection of foodborne pathogens. Viable pathogenic bacterial cells are a primary concern in processed foods, and bacteriophages can facilitate the monitoring and detection of viable pathogens because they can distinguish between viable and dead bacterial cells.[54] Bacteriophages possess high specificity and affinity for their hosts.[55] The specificity depends on nature and physiological assembly, localization, spatial configuration, and chemical composition of receptors on the bacterial surface. Excellent specificity is advantageous, especially in samples with a high non-target-to-target ratio. In addition, the developed biosensor did not require food or environmental samples to undergo pre-enrichment even for low-level inocula. Direct detection of viable targets and elimination of pre-treatment steps are significant improvements over traditional methods, which will mainly be advantageous for rapid on-site testing of samples. Last, a cocktail of bacteriophages is planned to be used in the future to simultaneously detect multiple targets in a single assay.

4. Conclusions

The detection of STEC strains has been generally based on traditional culture and immunological methods that take several days to complete. The novel, portable, and highly sensitive bacteriophage sandwich detection-based amperometric biosensor that allowed rapid and specific detection of viable STEC addressed the limitations of conventional approaches. In addition, biofunctionalized SPCEs with biotinylated bacteriophages offered tremendous flexibility in terms of performance and cost. Electrochemical analysis using a portable device that was wirelessly connected to a tablet proved the applicability of the sensor in on-site screening. Our sensor requires only a few simple steps prior to sample testing in microvolumes and has a turn-around time of less than 1 h. Further, it showed remarkable detection limits ($10–10^2$ CFU mL^{-1} or g) when applied to complex food samples, without the need for enrichment. The robustness and sensitivity of the biosensor were confirmed in testing natural environmental water samples by comparison with traditional plating and conventional PCR methods. This detection technology has great application potential in routine on-site STEC detection, in both pre- and post-harvest environments.

Conflicts of interest

There are no conflicts to declare.

Disclosure statement

The authors disclose that accompanying US Patent and Trademark Office (PTO) and Patent Cooperation Treaty (PCT) patent applications were filed. The patent applications USSN 16/115,97 and PCT/US19/47729 both comprised of the described bacteriophage-based biosensor technology.

Acknowledgements

The authors would like to thank Dr Yen-Te Liao at Produce Safety and Microbiology Research Unit, USDA ARS WRRC, for the isolation of STEC O179 bacteriophage. This work was supported by the United States Department of Agriculture (USDA NIFA AFRI) food safety grant (award number 2015-69003-23410) and the USDA-ARS CRIS projects 2030-42000-050-00D.

References

1 E. Vallières, M. Saint-Jean and F. Rallu, *J. Clin. Microbiol.*, 2013, **51**, 481–486.

2 L. Beutin and P. Fach, *Microbiol. Spectrum*, 2014, **2**, 3.
3 I. A. Quintela, B. G. de los Reyes, C.-S. Lin and V. C. Wu, *Nanoscale*, 2015, **7**, 2417–2426.
4 C. A. Fuller, C. A. Pellino, M. J. Flagler, J. E. Strasser and A. A. Weiss, *Infect. Immun.*, 2011, **79**, 1329–1337.
5 C. L. Mayer, C. S. Leibowitz, S. Kurosawa and D. J. Stearns-Kurosawa, *Toxins*, 2012, **4**, 1261–1287.
6 H. Trachtman, C. Austin, M. Lewinski and R. A. Stahl, *Nat. Rev. Nephrol.*, 2012, **8**, 658–669.
7 M. Rippa, R. Castagna, M. Pannico, P. Musto, G. Borriello, R. Paradiso, G. Galiero, S. Bolletti Censi, J. Zhou and J. Zyss, *ACS Sens.*, 2017, **2**, 947–954.
8 F. Mustafa, R. Hassan and S. Andreescu, *Sensors*, 2017, **17**, 2121.
9 N. Bhardwaj, S. K. Bhardwaj, M. K. Nayak, J. Mehta, K.-H. Kim and A. Deep, *Trends Anal. Chem.*, 2017, **97**, 120–135.
10 D. Wang, Q. Chen, H. Huo, S. Bai, G. Cai, W. Lai and J. Lin, *Food Control*, 2017, **73**, 555–561.
11 G. Ertürk and R. Lood, *Sens. Actuators, B*, 2018, **258**, 535–543.
12 A. K. Trilling, T. Hesselink, A. v. Houwelingen, J. H. G. Cordewener, M. A. Jongsma, S. Schoffelen, J. C. M. v. Hest, H. Zuilhof and J. Beekwilder, *Biosens. Bioelectron.*, 2014, **60**, 130–136.
13 N. Karoonuthaisiri, R. Charlermroj, U. Uawisetwathana, P. Luxananil, K. Kirtikara and O. Gajanandana, *Biosens. Bioelectron.*, 2009, **24**, 1641–1648.
14 K. M. Leach, J. M. Stroot and D. V. Lim, *Appl. Environ. Microbiol.*, 2010, **76**, 8044–8052.
15 Z.-Q. Shen, J.-F. Wang, Z.-G. Qiu, M. Jin, X.-W. Wang, Z.-L. Chen, J.-W. Li and F.-H. Cao, *Biosens. Bioelectron.*, 2011, **26**, 3376–3381.
16 N. Moll, E. Pascal, D. H. Dinh, J.-P. Pillot, B. Bennetau, D. Rebiere, D. Moynet, Y. Mas, D. Mossalayi and J. Pistré, *Biosens. Bioelectron.*, 2007, **22**, 2145–2150.
17 A. S. Afonso, B. Pérez-López, R. C. Faria, L. H. C. Mattoso, M. Hernández-Herrero, A. X. Roig-Sagués, M. Maltez-da Costa and A. Merkoçi, *Biosens. Bioelectron.*, 2013, **40**, 121–126.
18 A. M. Valadez, C. A. Lana, S.-I. Tu, M. T. Morgan and A. K. Bhunia, *Sensors*, 2009, **9**, 5810–5824.
19 Y. Zhao, H. Wang, P. Zhang, C. Sun, X. Wang, X. Wang, R. Yang, C. Wang and L. Zhou, *Sci. Rep.*, 2016, **6**, 21342.
20 B. J. Yakes, E. Papafragkou, S. M. Conrad, J. D. Neill, J. F. Ridpath, W. Burkhardt, M. Kulka and S. L. DeGrasse, *Int. J. Food Microbiol.*, 2013, **162**, 152–158.
21 A. Ben Aissa, J. J. Jara, R. M. Sebastián, A. Vallribera, S. Campoy and M. I. Pividori, *Biosens. Bioelectron.*, 2017, **88**, 265–272.
22 A. L. Bole and P. Manesiotis, *Adv. Mater.*, 2016, **28**, 5349–5366.
23 O. Lazcka, F. J. D. Campo and F. X. Muñoz, *Biosens. Bioelectron.*, 2007, **22**, 1205–1217.
24 H. Deng, Y. Xu, Y. Liu, Z. Che, H. Guo, S. Shan, Y. Sun, X. Liu, K. Huang and X. Ma, *Anal. Chem.*, 2012, **84**, 1253–1258.
25 V. Velusamy, K. Arshak, O. Korostynska, K. Oliwa and C. Adley, *Biotechnol. Adv.*, 2010, **28**, 232–254.
26 D. C. Vanegas, C. L. Gomes, N. D. Cavallaro, D. Giraldo-Escobar and E. S. McLamore, *Compr. Rev. Food Sci. Food Saf.*, 2017, **16**, 1188–1205.
27 A. Singh, S. Poshtiban and S. Evoy, *Sensors*, 2013, **13**, 1763–1786.
28 W. Sun, L. Brovko and M. Griffiths, *J. Ind. Microbiol. Biotechnol.*, 2000, **25**, 273–275.
29 E. Fernandes, V. Martins, C. Nóbrega, C. Carvalho, F. Cardoso, S. Cardoso, J. Dias, D. Deng, L. Kluskens and P. Freitas, *Biosens. Bioelectron.*, 2014, **52**, 239–246.
30 M. J. Loessner, M. Rudolf and S. Scherer, *Appl. Environ. Microbiol.*, 1997, **63**, 2961–2965.
31 H. M. Byeon, V. J. Vodyanoy, J.-H. Oh, J.-H. Kwon and M.-K. Park, *J. Electrochem. Soc.*, 2015, **162**, B230–B235.
32 Z. Wang, D. Wang, J. Chen, D. A. Sela and S. R. Nugen, *Analyst*, 2016, **141**, 1009–1016.
33 R. Edgar, M. McKinstry, J. Hwang, A. B. Oppenheim, R. A. Fekete, G. Giulian, C. Merril, K. Nagashima and S. Adhya, *Proc. Natl. Acad. Sci. U. S. A.*, 2006, **103**, 4841–4845.
34 L. Gervais, M. Gel, B. Allain, M. Tolba, L. Brovko, M. Zourob, R. Mandeville, M. Griffiths and S. Evoy, *Sens. Actuators, B*, 2007, **125**, 615–621.
35 Y.-H. Lin, S.-H. Chen, Y.-C. Chuang, Y.-C. Lu, T. Y. Shen, C. A. Chang and C.-S. Lin, *Biosens. Bioelectron.*, 2008, **23**, 1832–1837.
36 J. M. Denyes, M. Dunne, S. Steiner, M. Mittelviefhaus, A. Weiss, H. Schmidt, J. Klumpp and M. J. Loessner, *Appl. Environ. Microbiol.*, 2017, **83**, e00277-17.
37 J. D. Willford, B. Bisha, K. E. Bolenbaugh and L. D. Goodridge, *Bacteriophage*, 2011, **1**, 101–110.
38 J. Newman and K. E. Thomas-Alyea, *Electrochemical Systems*, John Wiley & Sons, 2012.
39 E. J. F. Dickinson, J. G. Limon-Petersen, N. V. Rees and R. G. Compton, *J. Phys. Chem. C*, 2009, **113**, 11157–11171.
40 N. m. Elgrishi, K. J. Rountree, B. D. McCarthy, E. S. Rountree, T. T. Eisenhart and J. L. Dempsey, *J. Chem. Educ.*, 2018, **95**, 197–206.
41 J.-Z. Tsai, C.-J. Chen, K. Settu, Y.-F. Lin, C.-L. Chen and J.-T. Liu, *Biosens. Bioelectron.*, 2016, **77**, 1175–1182.
42 Z. Hosseinidoust, T. G. M. Van de Ven and N. Tufenkji, *Langmuir*, 2011, **27**, 5472–5480.
43 E. Jończyk, M. Kłak, R. Międzybrodzki and A. Górski, *Folia Microbiol.*, 2011, **56**, 191–200.
44 A. R. Bennett, F. G. C. Davids, S. Vlahodimou, J. G. Banks and R. P. Betts, *J. Appl. Microbiol.*, 1997, **83**, 259–265.
45 Y. Zhou, A. Marar, P. Kner and R. P. Ramasamy, *Anal. Chem.*, 2017, **89**, 5735–5742.
46 R. Cademartiri, H. Anany, I. Gross, R. Bhayani, M. Griffiths and M. A. Brook, *Biomaterials*, 2010, **31**, 1904–1910.
47 L. Y. Zhang, R. Yuan, Y. Q. Chai and X. L. Li, *Anal. Chim. Acta*, 2007, **596**, 99–105.
48 X. Liu and D. K. Y. Wong, *Talanta*, 2009, **77**, 1437–1443.
49 X. Li, P. Zhu, C. Liu and H. Pang, *Chem. Commun.*, 2019, **55**, 9160–9163.
50 M. Yuan, X. Guo, N. Li, Q. Li, S. Wang, C.-S. Liu and H. Pang, *Sens. Actuators, B*, 2019, **297**, 126809.

51 P. Kuberský, A. Hamáček, S. Nešpůrek, R. Soukup and R. Vik, *Sens. Actuators, B*, 2013, **187**, 546–552.
52 J. Yao, X. Liu and K. Gillis, *Anal. Methods*, 2015, **7**, 5760–5766.
53 J. Yao and K. D. Gillis, *Analyst*, 2012, **137**, 2674–2681.
54 M. Zourob and S. Ripp, in *Recognition Receptors in Biosensors*, Springer, 2010, pp. 415–448.
55 A. Singh, D. Arutyunov, C. M. Szymanski and S. Evoy, *Analyst*, 2012, **137**, 3405–3421.